VIROLOGY 219, 190–194 (1996)
ARTICLE NO. 0236

Preliminary Crystallographic Studies of Bacteriophage T4 Fibritin Confirm a Trimeric Coiled-Coil Structure

SERGEI V. STRELKOV,*,† YIZHI TAO,* MICHAEL G. ROSSMANN,*,[1] LIDIYA P. KUROCHKINA,‡ MIKHAIL M. SHNEIDER,†,‡ and VADIM V. MESYANZHINOV†,‡

Department of Biological Sciences, Purdue University, West Lafayette, Indiana 47907; †The Ivanovsky Institute of Virology, 16 Gamaleya Str., 123098, Moscow, Russia; and ‡The Bakh Institute of Biochemistry, 33 Leninsky Prospect, 117071, Moscow, Russia

Received February 5, 1996; accepted March 6, 1996

Fibritin, a 52-kDa product of gene *wac* of bacteriophage T4, forms fibrous "whiskers" that connect to the phage tail and facilitate the later stages of phage assembly. Preliminary experiments suggest that fibritin is a trimer, and its predominant central part has a parallel α-helical coiled-coil structure. To investigate the oligomerization and function of fibritin, we have designed and studied two related deletion mutants, denoted M and E, that consist of its last 75 and 120 amino acids, respectively. Both proteins contain part of the coiled-coil region and the 29 amino acid carboxy-terminal domain essential for the trimerization of fibritin. The proteins are expressed as a soluble product in an *Escherichia coli* system. We have obtained crystals of fibritins M and E. Complete native X-ray diffraction data sets have been collected to 1.85 and 2.7 Å resolution, respectively. The crystals have space group *P*3 with $a = 44.3$ Å, $c = 91.3$ Å (fibritin M) and *R*32 with $a = 41.2$ Å, $b = 358.7$ Å (fibritin E) in the hexagonal setting. Symmetry and packing considerations show that fibritin is a triple coiled coil.

INTRODUCTION

Bacteriophage T4 is a double-stranded DNA virus which infects *Escherichia coli.* The T4 virion is formed by more than 40 different proteins and consists of two major structural elements: an icosahedral head and a contractile tail having sixfold symmetry (for a review, see Eiserling and Black, 1994). The tail baseplate, a hexagonal substructure located on the end of the tail opposite to the head, connects six long and six short tail fibers that are responsible for the recognition and attachment of the phage onto the host cell. Another set of six fibers, named whiskers, is connected to the phage tail at its junction with the head. The whiskers are formed by fibritin, a 52-kDa product of the nonessential gene *wac* expressed late in the viral life cycle, and play a role in the phage assembly, functioning as a specialized chaperonine. The whiskers, after being attached to the tail, probably interact with both proximal and distal parts of the unassembled long tail fibers. This interaction increases the rate of assembly of the long tail fibers and their subsequent attachment to the baseplate (Wood and Conley, 1979). The whiskers are also a simple sensing device that regulates the retraction of the long tail fibers in response to adverse environmental conditions (Conley and Wood, 1975).

Recombinant fibritin overexpressed in *E. coli* assembles into filamentous particles with a length of 530 Å. CD spectroscopy of these particles indicates a 90% α-helical content (Efimov *et al.,* 1994). The 486 amino acid sequence of fibritin consists of an amino-terminal domain (47 residues), a large central domain and a carboxy-terminal domain (29 residues). The central domain has 12 segments of various lengths, each containing heptad repeats $(a\text{-}b\text{-}c\text{-}d\text{-}e\text{-}f\text{-}g)_n$ where positions *a* and *d* are preferentially occupied by hydrophobic residues (Sobolev and Mesyanzhinov, 1991). Such a sequence pattern is characteristic for coiled-coil proteins (McLachlan and Stewart, 1975; Cohen and Parry, 1990). The segments are connected by short linker regions where the heptad periodicity is broken (Fig. 1). Further biophysical and sequence analysis has led to a model of fibritin as a parallel triple-stranded α-helical coiled coil (Efimov *et al.,* 1994).

The amino- and carboxy-terminal domains of fibritin have no heptad repeats and their structure is probably different from that of a coiled coil. Mutant fibritin, lacking residues at the amino terminus, assembles correctly but fails to attach to the phage tail (Efimov *et al.,* 1994). In contrast, the carboxy-terminal domain is necessary for correct assembly of fibritin trimers *in vitro,* because deletions in the carboxy-terminal domain yield an insoluble expression product similar to inclusion bodies (Efimov *et al.,* 1994).

The structure of fibritin is convenient for studying the mechanisms that define protein stability as well as the pathway of protein folding and oligomerization. Furthermore, foreign polypeptides can be expressed

[1] To whom correspondence and reprint requests should be addressed.

0042-6822/96 $18.00

FIG. 1. Amino acid sequences of wild-type fibritin and mutants M and E. Small letters denote residues different from the wild-type fibritin sequence. The putative coiled-coil region is indicated by heptad repeats (abcdefg) where the bold letters are the positions that favor hydrophobic residues. Dashes (-----) indicate loops connecting the coiled-coil segments.

on the surface of phage T4 by fusing them to the carboxy terminus of fibritin (Efimov *et al.,* 1995). Similar to the recently devised phage lambda vector (Maruyama *et al.,* 1994), a surface-expressing vector based on phage T4 might be useful for the display of proteins that cannot be secreted.

We have initiated structural studies of recombinant fibritin in order to investigate the phage assembly. It has not yet been possible to crystallize the full-length wild-type fibritin. Therefore, two deletion mutants, fibritins M and E, which consist of the last 75 and 120 amino acid residues of the wild-type fibritin, respectively, have been constructed. They have only 1 and 3 putative coiled-coil segments encompassing 6 and 10 full heptad repeats, respectively, together with the complete carboxy-terminal domain. In addition, fibritin M has several substitutions with respect to the wild-type sequence that were introduced to further facilitate the formation of a coiled coil. A hydrophilic residue in a *d* position has been replaced by a hydrophobic one and additional favorable pairs of oppositely charged side chains have been introduced according to the principles proposed by Cohen and Parry (1990). Both fibritins M and E have been expressed, in soluble form, in an *E. coli* system. Here, we present the successful crystallizations and preliminary X-ray crystallographic analyses of fibritins M and E.

MATERIALS AND METHODS

Construction of plasmids encoding fibritins M and E, expression, and purification

Polymerase chain reaction (PCR) was used to generate DNA fragments encoding truncated fibritins. Two oligonucleotide forward-primers (Table 1) were used to obtain a *Nco*I restriction site (CCATGG) and to generate f-Met residues within the *wac* gene. A back-primer (Table 1) was used to produce a *Bam*HI restriction site (GGATCC) downstream of the *wac* gene sequence. The forward-primer, *wac*-M, was designed to make several substitutions in the *wac* gene. The DNA fragments obtained encode polypeptides of 75 amino acids (fibritin M) and 120 amino acids (fibritin E) (Fig. 1). In both cases, the N-terminal methionine is probably not present in the expressed product.

Amplification of the fragments was done from the pWAC plasmid (Efimov *et al.,* 1994), which expresses the full-length fibritin. Twenty PCR cycles were used. After digestion with *Nco*I and *Bam*HI enzymes, the purified

TABLE 1

Primers Used for Construction of Mutant Fibritins

Forward-primers:
wac-M
5′-CCA AAC GGT TCC ATG GTT GAA GAG AGC GGA TTA ACC AAT AAA ATA AAA GCT ATC GAA ACT GAT ATT GCA TCA GTT AGA CAA
wac-E
5′-CGA GTT TCT ACC ATG GAA ACT
Back-primer:
5′-AAT TGG ATC CCC TAA ACG TCT

PCR fragments were cloned into the Pet19B vector (Novagen) under the phage T7 promoter. The plasmids were expressed in *E. coli* strain BL21 (DE3) as described by Studier *et al.* (1990).

Purification of recombinant fibritins was performed as described by Efimov *et al.* (1994). For an effective salting-out step during purification, the ammonium sulfate concentration had to be adjusted to 45 and 30% saturation for fibritins M and E, respectively, thus showing the difference in their solubility properties. The proteins were about 95% pure judging from the polyacrylamide gel electrophoresis in the presence of sodium dodecyl sulfate stained with Coomassie blue.

Crystallization and X-ray diffraction studies

Fibritins M and E were crystallized by the hanging drop, vapor diffusion method. The best crystals of fibritin M were grown using 1.75 *M* Li_2SO_4 in 0.1 *M* Tris–HCl buffer at pH 7.5 as a precipitant. The crystallization drops were made by mixing 6 μl of protein solution (20 mg/ml in 10 m*M* Na phosphate buffer, pH 7.5) with an equal volume of the precipitant solution and equilibrated against the same precipitant solution in the well. Plate-like crystals of about 0.35 × 0.35 × 0.07 mm could be reproducibly obtained after 3 days at 18°. The crystals clearly show a threefold axis perpendicular to the plane of the plate. The minimal concentration of Li_2SO_4 that yielded crystals was 1.5 *M*. Under these conditions, the crystals had a very uniform shape, but their thickness did not exceed 0.02 mm. Increasing the precipitant concentration (up to 1.85 *M* Li_2SO_4) resulted in thicker crystals, but also in more rapid growth and occasional morphological imperfections. Small single crystals could also be obtained from $(NH_4)_2SO_4$, Na, K tartrate, and Na citrate.

The best fibritin E crystals were obtained at 22° using 34% PEG400, 0.1 *M* $Zn(COOH)_2$ in 0.1 *M* MES buffer at pH 6.0 as well solution, and using 1 μl well solution mixed with 1.2 μl protein solution (29 mg/ml) in the drop. Rhombohedral crystals, about 0.6 mm in length, grew in about 3 days. Variations of crystallization conditions, such as (1) PEG600 instead of PEG400; (2) buffer at pH 4.5, 5.0, 5.5, or 6.5 instead of pH 6.0; (3) addition of β-octyl glucoside, were explored but produced smaller and irregular-shaped crystals.

The crystals of fibritins M and E were exposed to CuK_α radiation ($\lambda = 1.5418$ Å) from a Rigaku rotating anode X-ray source, operated at 50 kV and 100 mA, equipped with perpendicular focusing mirrors, a Ni filter, and a helium path. Oscillation images were recorded by an R-axis IIc image plate detector (Molecular Structure Corp.). The data sets (Table 2) were processed using the programs DENZO and SCALEPACK (Otwinowski, 1993).

The fibritin M crystals showed radiation damage after

TABLE 2

Summary of Crystallographic Data on Fibritins M and E

	Fibritin M	Fibritin E
Temperature of data collection	100°K	298°K
Resolution limits	30–1.85 Å	40–2.7 Å
No. of observations, including partially recorded reflections	39783	18747
No. of unique reflections	14861	3575
Completeness[a]	89.8% (53.6%)	99.6% (100%)
R_{merge}[a,b]	0.036 (0.182)	0.059 (0.186)
Space group and cell dimensions	*P*3 *a* = 43.7 Å, *c* = 90.6 Å (*a* = 44.3, *c* = 91.3 at room temperature)	*R*32 *a* = 41.2 Å, *c* = 358.7 Å (hexagonal setting)
No. of monomers per asymmetric unit	3 or 2	1
V_M[c]	2.15 Å^3/Da[d] 3.23 Å^3/Da[e]	2.35 Å^3/Da

[a] The data in parentheses are for the highest resolution bin, 1.92–1.85 Å (fibritin M) and 2.75–2.70 Å (fibritin E).
[b] $R_{merge} = \sum_h \sum_i |I_{hi} - \langle I_h \rangle| / \sum_h \sum_i I_{hi}$
[c] At room temperature.
[d] Assumes three monomers per asymmetric unit.
[e] Assumes two monomers per asymmetric unit.

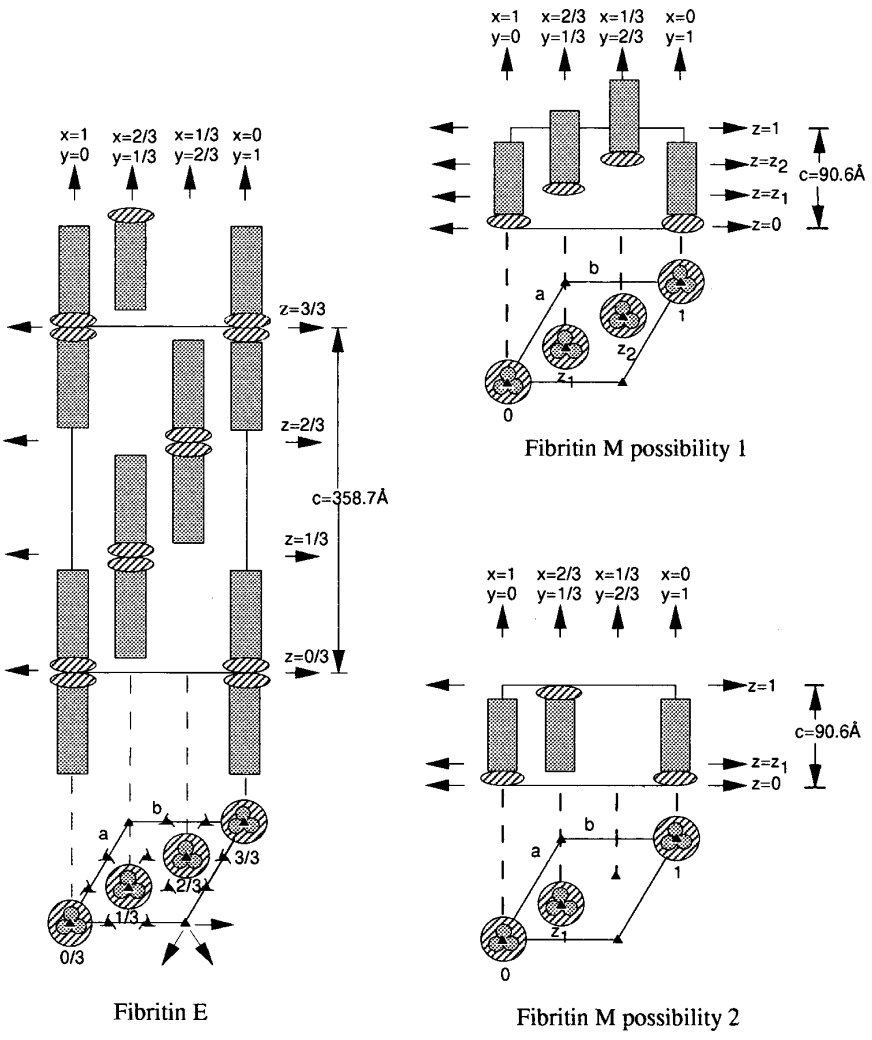

FIG. 2. Possible packing arrangements for fibritin E and fibritin M. The fibritin molecule fragment is a trimer with each monomer having a carboxy-terminal domain and a trimeric coiled-coil fiber. Each trimeric molecule when viewed sideways is shown as a shaded cylinder (representing an α-helical coiled coil) plus a hatched elliptical shape (representing the carboxy-terminal domain). In the top view down the threefold axes, the trimeric molecule is shown as a shaded clover-leaf structure superimposed onto the slightly larger diameter hatched carboxy-terminal domain. Fibritin M has a shorter fiber than fibritin E. The scale of the *c* axis is shortened relative to the scale of the *a* and *b* axes. The space group *R*32 of fibritin E (left) leaves little doubt about the packing organization. However, the space group *P*3 for fibritin M permits two possibilities. In 1 (top right), there are three parallel molecules equally distributed in the cell. In 2 (bottom right), there are two antiparallel molecules whose orientation and packing are similar to that of fibritin E.

several hours of continuous exposure at room temperature. They could be flash-frozen on a hair loop in a nitrogen gas jet at 100°K after being soaked in a solution containing glycerol. The glycerol had been increased gradually to a final concentration of 25% (v/v) in 0.06 *M* Tris–HCl buffer, pH 7.5, containing 1.45 *M* Li_2SO_4, over a period of 1 hr. A total of 103 consecutive oscillation images (10 min exposure and 1° rotation per image) were recorded from a single flash-frozen crystal.

The diffraction data for the fibritin E crystals were collected at room temperature as no significant radiation decay was observed during the time of data collection. A total of 95 oscillation images (12 min exposure, 1° rotation per image) were recorded from a single crystal.

RESULTS AND DISCUSSION

The V_M value (Matthews, 1968) for the fibritin E crystals is 2.35 Å^3/dalton, assuming one molecule per crystallographic asymmetric unit. Therefore, considering the propensity for the fibritin monomer to oligomerize, there are six trimers per unit cell, each curled around a threefold axis (Fig. 2). The V_M value for the fibritin M crystals is 2.15 or 3.23 Å^3/dalton, assuming 3 or 2 monomers per crystallographic asymmetric unit, respectively. As the *a* and *b* axes are essentially the same lengths for the fibritin E hexagonal and fibritin M trigonal unit cells, with the same distribution of crystallographic threefold axes, it follows that the packing of the trimers in the fibritin E and M crystal forms is likely to be similar. The distance

between trimers is about 25 Å, which is a reasonable outer diameter for a triple coiled coil. There are two possible packing arrangements for fibritin M: the first would have three parallel trimers maintaining the lateral packing between trimers on each threefold axis; the second would have two antiparallel trimers per cell, which maintain the same interaction between neighboring molecules as in fibritin E (Fig. 2).

Trimeric structures in fibrous components of viruses are usual. Other examples are the short tail fibers of phage T4 (Mason and Haselkorn, 1972; Makhov *et al.,* 1993), although probably composed of β structure; long T4 tail fibers (Cerritelli *et al.,* 1994); phage P22 spike protein (Steinbacher *et al.,* 1994); the tail fiber protein of the related phages T7 (Steven *et al.,* 1988) and T3 (Takahashi and Ooi, 1988); influenza virus hemagglutinin (Wilson *et al.,* 1981); coronavirus spike protein (de Groot *et al.,* 1987; Delmas and Laude, 1990); reovirus cell attachment protein (Leone *et al.,* 1992); and adenovirus fiber protein (Stouten *et al.,* 1992; Xia *et al.,* 1994).

A search for suitable heavy atom derivatives is now in progress.

ACKNOWLEDGMENTS

We are grateful for helpful advice from Terje Dokland, Prasanna Kolatkar, Sukyeong Lee, Guoguang Lu, and Cory Momany. This work was supported by a grant from the National Science Foundation to M.G.R., and also by a grant from the Protein Engineering Council, Russia, and in part by Grant No. 93-04-07024 from the Russian Foundation of Basic Research to V.V.M. V.V.M. is an International Howard Hughes Medical Institute Scholar and holds a collaborative International HHMI grant with M.G.R.

REFERENCES

Cerritelli, M. E., Simon, M. N., Vaca, M., Conway, J. F., and Steven, A. C. (1994). The long tail-fibers of bacteriophage T4: Determination of stoichiometry and domainal structure by dark-field STEM. Proceedings of the 13th International Congress on Electron Microscopy, Volume 3A, Paris, France.

Cohen, C., and Parry, D. A. D. (1990). α-helical coiled coils and bundles: How to design an α-helical protein. *Proteins* 7, 1–15.

Conley, M. P., and Wood, W. B. (1975). Bacteriophage T4 whiskers: A rudimentary environment-sensing device. *Proc. Natl. Acad. Sci. USA* 72, 3701–3705.

de Groot, R. J., Luytjes, W., Horzinek, M. C., van der Zeijst, B. A. M., Spaan, W. J. M., and Lenstra, J. A. (1987). Evidence for a coiled-coil structure in the spike proteins of coronaviruses. *J. Mol. Biol.* 196, 963–966.

Delmas, B., and Laude, H. (1990). Assembly of coronavirus spike protein into trimers and its role in epitope expression. *J. Virol.* 64, 5367–5375.

Efimov, V. P., Nepluev, I. V., and Mesyanzhinov, V. V. (1995). Bacteriophage T4 as a surface expression vector. *Virus Genes* 10, 173–177.

Efimov, V. P., Nepluev, I. V., Sobolev, B. N., Zurabishvili, T. G., Schulthess, T., Lustig, A., Engel, J., Haener, M., Aebi, U., Venyaminov, S. Y., Potekhin, S. A., and Mesyanzhinov, V. V. (1994). Fibritin encoded by bacteriophage T4 gene *wac* has a parallel triple-stranded α-helical coiled-coil structure. *J. Mol. Biol.* 242, 470–486.

Eiserling, F. A., and Black, L. W. (1994). Pathways in T4 morphogenesis. In "Molecular Biology of Bacteriophage T4" (Karam, E., Ed.), pp. 209–212. American Soc. Microbiol., Washington, DC.

Leone, G., Maybaum, L., and Lee, P. W. K. (1992). The reovirus cell attachment protein possesses two independently active trimerization domains: Basis of dominant negative effects. *Cell* 71, 479–488.

Makhov, A. M., Trus, B. L., Conway, J. F., Simon, M. N., Zurabishvili, T. G., Mesyanzhinov, V. V., and Steven, A. C. (1993). The short tail-fiber of bacteriophage T4: Molecular structure and a mechanism for its conformational transition. *Virology* 194, 117–127.

Maruyama, I. N., Maruyama, H. I., and Brenner, S. (1994). λfoo: A λ phage vector for the expression of foreign proteins. *Proc. Natl. Acad. Sci. USA* 91, 8273–8277.

Mason, W. S., and Haselkorn, R. (1972). Product of T4 gene 12. *J. Mol. Biol.* 66, 445–469.

Matthews, B. W. (1968). Solvent content of protein crystals. *J. Mol. Biol.* 33, 491–497.

McLachlan, A. D., and Stewart, M. (1975). Tropomyosin coiled-coil interactions: Evidence for an unstaggered structure. *J. Mol. Biol.* 98, 293–304.

Otwinowski, Z. (1993). DENZO. In "Data Collection and Processing" (Sawyer, L., Isaacs, N., and Bailey, S., Eds.), pp. 56–62. SERC Daresbury Laboratory, Warrington, UK.

Sobolev, B. N., and Mesyanzhinov, V. V. (1991). The *wac* gene product of bacteriophage T4 contains coiled-coil structure patterns. *J. Biomol. Struct. Dynam.* 8, 953–965.

Steinbacher, S., Seckler, R., Miller, S., Steipe, B., Huber, R., and Reinemer, P. (1994). Crystal structure of P22 tailspike protein: Interdigitated subunits in a thermostable trimer. *Science* 265, 383–386.

Steven, A. C., Trus, B. L., Maizel, J. V., Unser, M., Parry, D. A. D., Wall, J. S., Hainfeld, J. F., and Studier, F. W. (1988). Molecular substructure of a viral receptor-recognition protein. The gp17 tail-fiber of bacteriophage T7. *J. Mol. Biol.* 200, 351–365.

Stouten, P. F. W., Sander, C., Ruigrok, R. W. H., and Cusack, S. (1992). New triple-helical model for the shaft of the adenovirus fiber. *J. Mol. Biol.* 226, 1073–1084.

Studier, F. W., Rosenberg, J. J., Dunn, J. J., and Dubendorff, J. W. (1990). Use of T7 RNA polymerase to direct expression of cloned genes. *Methods Enzymol.* 185, 60–89.

Takahashi, S., and Ooi, T. (1988). Three α-helical coiled-coil, as a proposed model for a thin rod segment of bacteriophage T3 tail fibers. *Biochem. Biophys. Res. Commun.* 150, 1244–1250.

Wilson, I. A., Skehel, J. J., and Wiley, D. C. (1981). Structure of the haemagglutinin membrane glycoprotein of influenza virus at 3 Å resolution. *Nature (London)* 289, 366–373.

Wood, W. B., and Conley, M. P. (1979). Attachment of tail fibers in bacteriophage T4 assembly. *J. Mol. Biol.* 127, 15–29.

Xia, D., Henry, L. J., Gerard, R. D., and Deisenhofer, J. (1994). Crystal structure of the receptor-binding domain of adenovirus type 5 fiber protein at 1.7 Å resolution. *Structure* 2, 1259–1270.